UNIVERSITY
OF TASMANIA

3D Printed Miniaturised Analytical Devices

(3D MADe)

Vipul Gupta

B.Pharm, MS

School of Physical Sciences

A dissertation submitted in partial fulfilment of the requirements for the

Doctor of Philosophy

(Chemical Sciences)

University of Tasmania

January 2018

Declaration of Originality

This thesis contains no material which has been accepted for a degree or diploma by the University or any other institution, except by way of background information and duly acknowledged in the thesis, and to the best of my knowledge and belief no material previously published or written by another person except where due acknowledgement is made in the text of the thesis, nor does the thesis contain any material that infringes copyright.

Authority of Access

This thesis may be made available for loan and limited copying and communication in accordance with the Copyright Act 1968.

Statement regarding published work contained in thesis

The publishers of the papers comprising Chapters 2 to 5 hold the copyright for that content, and access to the material should be sought from the respective journals. The remaining non published content of the thesis may be made available for loan and limited copying and communication in accordance with the Copyright Act 1968.

Statement of Co-Authorship

The following people and institutions contributed to the publication of work undertaken as part of this thesis:

Vipul Gupta, Australian Centre for Research on Separation Science (ACROSS) and ARC Centre of Excellence for Electromaterials Science, School of Physical Sciences, University of Tasmania, Australia = **Candidate**

Brett Paull, Australian Centre for Research on Separation Science (ACROSS) and ARC Centre of Excellence for Electromaterials Science, School of Physical Sciences, University of Tasmania, Australia = **Author 1 (Primary Supervisor)**

Pavel N. Nesterenko, Australian Centre for Research on Separation Science (ACROSS), School of Physical Sciences, University of Tasmania, Australia = **Author 2 (Co-Supervisor)**

Gordon G. Wallace, ARC Centre of Excellence for Electromaterials Science, Intelligent Polymer Research Institute, University of Wollongong, Australia = **Author 3**

Sara Sandron, Australian Centre for Research on Separation Science (ACROSS), School of Physical Sciences, University of Tasmania, Australia = **Author 4**

Brendan Heery, *Australian Centre for Research on Separation Science (ACROSS), School of Physical Sciences, University of Tasmania, Australia* = **Author 5**

Stephen Beirne, ARC Centre of Excellence for Electromaterials Science, Intelligent Polymer Research Institute, University of Wollongong, Australia = **Author 6**

Mohammad Talebi, Australian Centre for Research on Separation Science (ACROSS), School of Physical Sciences, University of Tasmania, Australia = **Author 7**

Fletcher Thompson, *Australian Centre for Research on Separation Science (ACROSS), School of Physical Sciences, University of Tasmania, Australia* = **Author 8**

Jeremy Deverell, *Australian Centre for Research on Separation Science (ACROSS), School of Physical Sciences, University of Tasmania, Australia* = **Author 9**

David A. Collins, *Marine Environmental Sensing Technology Hub (MESTECH), Dublin City University, Ireland* = **Author 10**

Ekaterina P. Nesterenko, *Marine Environmental Sensing Technology Hub (MESTECH), Dublin City University, Ireland* = **Author 11**

Dermot Brabazon, *Advanced Processing Technology Research Centre, Dublin City University, Ireland*= **Author 12**

Fiona Regan, *Marine Environmental Sensing Technology Hub (MESTECH), Dublin City University, Ireland* = **Author 13**

Parvez Mahbub, Australian Centre for Research on Separation Science (ACROSS), School of Physical Sciences, University of Tasmania, Australia = **Author 14**

Author details and their roles:

Paper 1, 3D printed metal columns for capillary liquid chromatography:

Located in Chapter 2

Candidate performed most of the experimental investigation and contributed to the formalisation, development, and presentation of the work. (Approximate candidate contribution to the total work = 40%)
Author 1 and author 2 contributed to the inception of the idea and formalisation, development, and presentation of the work
Author 3, author 10, author 11, author 12, and author 13 contributed to the inception of the idea
Author 4 and author 5 performed the preliminary investigation and contributed to the formalisation, development, and presentation of the work
Author 6, author 7, and author 8 offered general laboratory assistance

Paper 2, 3D printed titanium micro-bore columns containing polymer monoliths for reversed-phase liquid chromatography:

Located in Chapter 3

Candidate performed all the experimental investigation, and with author 1, author 2, and author 3 contributed to the inception of the idea and to the formalisation, development, and presentation of the work. (Approximate candidate contribution to the total work = 75%)

Author 4, author 5, author 6, author 7, author 8, and author 9 offered general laboratory assistance

Paper 3, Investigating the effect of column geometry on separation efficiency using 3D printed liquid chromatographic columns containing polymer monolithic phases:

Located in Chapter 4

Candidate performed all the experimental and theoretical investigation, and with author 1, author 2, and author 3 contributed to the inception of the idea and to the formalisation, development, and presentation of the work. (Approximate candidate contribution to the total work = 75%)

Author 6 offered general laboratory assistance

Paper 4, A new 3D printed radial flow-cell for chemiluminescence detection: Application in ion chromatographic determination of hydrogen peroxide in urine and coffee extracts:

Located in Chapter 5

Candidate performed all the experimental and theoretical investigation, and with author 1, author 2, and author 3 contributed to the inception of the idea and to the formalisation, development, and presentation of the work. (Approximate candidate contribution to the total work = 75%)

Author 14 offered general laboratory assistance

We the undersigned agree with the above stated "proportion of work undertaken" for each of the above published (or submitted) peer-reviewed manuscripts contributing to this thesis:

Signed:

Prof. Brett Paull
Supervisor
School of Natural Sciences
University of Tasmania

Prof. Mark Hunt
Head of School
School of Natural Sciences
University of Tasmania

Date: 18 July 2018 19/7/18

ACKNOWLEDGEMENT

I would like to extend my sincere thanks to my advisors, friends, and family members for all their help, support, and encouragement throughout my doctoral and pre-doctoral studies to enable me today to present this thesis.

I cannot express enough thanks to my PhD supervisors Prof. Brett Paull and Prof. Pavel N. Nesterenko to give me an opportunity to work under their guidance, be available at every step of the PhD, always provide useful advice, and be always supportive and encouraging towards my attempts to try new ideas and projects. They have always encouraged my personal and scientific growth by allowing me to explore new avenues and opportunities and guiding my way throughout the process. I would also like to thank my Masters' Degree supervisor Prof. Matthew R. Linford for training me and guiding me through the basic elements of scientific research and for his valuable advice during several PhD projects.

This interdisciplinary work would not have been possible without a close collaboration with various individuals, namely Gordon G. Wallace, Stephen Beirne, Fletcher Thompson, Parvez Mahbub, Tom Kazarian, Mohammad Talebi, Sara Sandron, Brendan Heery, Jeremy Deverell, David A. Collins, Ekaterina P. Nesterenko, Dermot Brabazon, and Fiona Regan. I would like to thank them all for their help and support during respective projects.

I would like to express my gratitude to the financial support provided by the University of Tasmania, Tasmanian Graduate Research Scholarship (TGRS), Australian Research Council (Grant number CE140100012), and additive fabrication facilities provided by the Australian National Fabrication Facility (ANFF) Materials Node.

I am grateful to Prof. Jason A Smith, Murray Frith, Dr. Petr Smejkal, Jennifer Nield, and Patricia McKay for all their help and support during various laboratory and administrative

operations. I would like to extend my sincere thanks to Prof. Charles Lucy, Prof. Joe Foley, Dr Kevin Thomas, and Paul Worsfold for having a healthy discussion and providing me with valuable guidance during their visit to the Australian Centre for Research on Separation Science (ACROSS).

I thank my friends Benjamin Savarear, Manish Khandagale, Chowdhury Kamrul Hasan, Mohammad Rahbar, Sumit Sahni, and Tushar Tomar for their help and advice on various occasions.

Most importantly, I would like to thank my family; my wife (Arushi Manchanda Gupta), my parents (Mrs. Brij Bala Gupta and Mr Pushkar Gupta), my in-laws (Mrs. Arti Manchanda and Dr Subhash Manchanda), and my brother (Mohit Gupta) for their undying support, never-ending encouragement, making me laugh when I am sad, picking me up when I am down, and standing with me during each sad and happy phase of my life. None of this would have been possible without their love and support.

ABSTRACT

3D printing has gained popularity in almost every field of research, development, and manufacturing due to its ability to fabricate complex three-dimensional prototypes and functional devices with relative ease, which was unimaginable in the past. Herein, different 3D printing techniques have been studied to understand their capabilities and potential to miniaturise and increase the performance of analytical devices. In particular, selective laser melting and PolyJet 3D printing techniques have been used to develop new functional 3D printed miniaturised analytical devices with three-dimensional micro- and milli-fluidic channels.

An initial study was undertaken to assess the ability of selective laser melting technique to fabricate 600 mm long, 0.9 mm I.D. stainless steel (316L) and titanium alloy (Ti-6Al-4V) columns within a footprint of 5 × 30 × 30 mm. The 3D printed stainless steel column was slurry packed with octadecyl silica particles, and it was used for liquid chromatographic separations of small molecules. This study provided a proof of concept for the use of selective laser melting technique to fabricate miniaturised metallic capillary liquid chromatographic columns. However, these 3D printed columns resulted in a channel wall roughness of 20 μm, which limited the chromatographic performance of the slurry packed liquid chromatographic columns. Accordingly, the 3D printed titanium column was functionalised with in-column thermally polymerised poly(butyl methacrylate-*co*-ethylene glycol dimethacrylate) (BuMA-*co*-EDMA) monolith to circumvent the limitation of channel wall roughness. Silanisation of thermally oxidised titanium channel walls allowed a successful covalent wall bonding between the titanium column and the acrylate monolith.

The prepared monolithic column was successfully used for reversed-phase liquid chromatographic (RPLC) separations of intact proteins and peptides. The use of a Peltier thermoelectric module based heating/cooling system allowed the generation of rapid temperature gradients to further improve the RPLC separations of the intact proteins.

The initial study was then extended to explore the ability of 3D printing techniques to design and fabricate geometrically complex 3D column geometries. Three different column geometries were designed and 3D printed in titanium, namely 2D serpentine, 3D spiral, and 3D serpentine. These columns were used to perform an investigation into the effect of 3D column geometry on the liquid chromatographic efficiencies of monolithic columns. All three columns allowed successful in-column thermal polymerisation of mechanically stable and uniform poly(BuMA-*co*-EDMA) monoliths. Van Deemter plots indicated higher liquid chromatographic efficiencies of the chromatographic columns with higher aspect ratio turns at higher linear velocities and smaller analysis time as compared to their counterpart columns with lower aspect ratio turns. Computational fluid dynamic (CFD) simulations of a basic monolithic structure indicated 44%, 90%, 100%, and 118% higher flow through narrow channels in the curved monolithic configuration as compared to the straight monolithic configuration at linear velocities of 1 mms^{-1}, 2.5 mms^{-1}, 5 mms^{-1}, and 10 mms^{-1}, respectively. An improvement in the interaction between wide and narrow channels in high aspect ratio coiled columns offers a possible explanation behind the above-mentioned trends in the Van Deemter plots. Use of the highly convoluted 3D serpentine column at higher flow rates as compared to the less convoluted 3D spiral column allowed 58% reduction in the analysis time and 74% increase in the peak capacity for the isocratic separations of the small molecules and the gradient separations of the proteins, respectively.

In addition to the use of the selective laser melting 3D printing technique to fabricate metallic miniaturised analytical devices, the use of the PolyJet 3D printing technique was also explored to fabricate polymeric miniaturised analytical devices. The PolyJet 3D printing technique was successfully used to fabricate a new transparent polymer radial flow-cell for chemiluminescence detection (CLD). The PolyJet 3D printed radial flow-cell resulted in an increase in both the signal magnitude and duration for CLD of H_2O_2. The new flow-cell design provided an average increase in the peak height of 63% and 58%, in peak area of 89% and 90%, and in peak base width of 41% and 42%, as compared to its coiled-tubing spiral flow-cell and PolyJet 3D printed spiral flow-cell, respectively. CFD simulations indicated that the higher spatial coverage near the inlet and the lower linear velocities in the radial flow-cell could be contributing towards its higher signal magnitude and higher signal duration, respectively. The PolyJet 3D printed radial flow-cell was applied within a developed selective, sensitive, and reproducible ion chromatography coupled chemiluminescence detection (IC-CLD) assay for the determination of H_2O_2 (a biomarker) in urine and coffee extract samples.

TABLE OF CONTENTS

LIST OF FIGURES

Chapter 1

Chapter 2

Chapter 3

Chapter 5

List of Tables

Chapter 5

LIST OF ABBREVIATIONS

3D MADe:	3D printed miniaturised analytical devices
BuMA-*co*-EDMA:	poly(butyl methacrylate-co-ethylene glycol dimethacrylate)
PS-DVB:	poly(styrene-co-divinylbenzene)
RPLC:	reversed-phase liquid chromatography
HPLC:	high-performance liquid chromatography
GC:	gas chromatography
CE:	capillary electrophoresis
CZE:	capillary zone electrophoresis
CFD:	computational fluid dynamic
CLD:	chemiluminescence detection
IC-CLD:	ion chromatography coupled chemiluminescence detection
SL:	stereolithography
SLS:	selective laser sintering
SLM:	selective laser melting
FDM:	fused deposition modeling
ABS:	acrylonitrile butadiene styrene
PLA:	poly(lactic acid)
SS:	stainless steel
FSC:	fused silica capillary
ϒ-MAPS:	3-trimethoxysilylpropyl methacrylate
AIBN:	azobisisobutyronitrile
PTFE:	polytetrafluoroethylene
ODS:	octadecyl silica
RNase A:	ribonuclease A
Ti:	trypsin inhibitor
Cyc:	cytochrome c
Lys:	lysozyme
Trg:	trypsinogen

α-Lal:	α-lactalbumin
Tf:	transferrin
My:	myoglobin
β-Lac:	β -lactoglobulin
PTM:	Peltier thermoelectric module
PID:	proportional–integral–derivative
UNF:	unified fine pitch threads
RANS:	Reynolds-averaged Navier-Stokes
SST:	shear stress transport
FIA:	flow injection analysis
PMT:	photomultiplier tube
FOX:	ferrous oxidation-xylenol orange
3DP RFC:	3D printed radial flow-cell
SFC:	spiral flow-cell
3DP SFC:	3D printed spiral flow-cell
E.Coli:	Escherichia coli

Chapter 1:

INTRODUCTION

The miniaturisation of analytical devices continues to receive significant research interest, because of the widespread potential of such miniaturised analytical devices in various applications, which in recent times has included real-time environmental monitoring[1-2], detection of explosives and other warfare agents at sensitive sites[3], personal medical diagnosis[4], and online monitoring of various processes parameters and hazards[5]. The production of these functional miniaturised analytical devices often requires fabrication of three-dimensionally oriented micro- and milli-fluidic channels. However, conventional manufacturing techniques, such as photolithography, milling, etching, and injection moulding demand alignment and bonding of multiple components to achieve these goals. This renders the conventional fabrication process cumbersome, and often inefficient in terms of the time and cost. Moreover, lithographic techniques require (1) the use of hazardous chemicals, (2) long processing times, (3) expensive clean-room facilities, and (4) highly skilled labour. A relatively recent technology that looks set to revolutionise such procedures is that of 3D printing. 3D printing techniques can offer (1) the ability to directly fabricate complex three-dimensionally oriented geometries, (2) cost and time effective production, (3) relative ease of use, (4) minimisation of the material wastage, (5) hazardous chemicals free procedure, (6) a "fail fast and often"[6] approach for prototyping, customisation, and testing, and (7) the production of monolithically integrated devices. This makes 3D printing a potentially highly useful new approach for fabricating functional miniaturised analytical devices.

3D printing was first patented by Charles Hull in 1986[7], and following its introduction, this technique has been extensively used in almost all fields of research and manufacturing, such as biotechnology and life sciences[8-9], engineering[10], robotics[11], arts[12], and food sciences[13], to name but a few. Whitesides group reported the first use of a 3D printing technique (PolyJet printing) to fabricate three-dimensional microfluidic devices[14] in 2002. Since then different 3D printing techniques have been increasingly used in the wider fields of chemical sciences[15].

Types of 3D Printing Techniques

The most commonly and widely used 3D printing techniques to-date are stereolithography (SL), inkjet printing, selective laser sintering (SLS), and fused deposition modeling (FDM). The details and principles behind each of these techniques are compared and contrasted in Table 1. Apart from the above-listed techniques, other less commonly used 3D printing techniques include, but are not limited to, laminated object manufacturing, two-photon lithography, micro-3D writing, and direct-ink writing. In this research work, two of the above-mentioned 3D printing techniques, namely SLS and inkjet printing were used, which are individually described in detail below.

Table 1. Properties of the stereolithography, inkjet printing, selective laser sintering, and fused deposition modeling 3D printing techniques.

	Stereolithography (SL)	**Inkjet Printing**	**Selective Laser Sintering (SLS)**	**Fused Deposition Modeling (FDM)**
Synonyms	Digital Light Projection (DLP), Stereolithographic Apparatus (SLA)	PolyJet Printing/Modeling, MultiJet Printing/Modeling (MJM), Drop On Demand (DOD), Thermo Jetting, Binder Jetting, 3D printing	Selective Laser Melting (SLM), Direct Metal Laser Sintering (DMLS), Laser Curing	Fused Filament Fabrication (FFF), Thermoplastic Extrusion, Fused Layer Modeling/Manufacturing (FLM)
Principle	Photopolymerisation of a liquid photopolymer by direct laser writing or mask-based laser writing to form each individual layer.	Spatially controlled jetting of a binder, a photopolymer, or a thermomaterial, which bonds powder particles together, photopolymerises, or solidifies, respectively to form each individual layer.	Laser selectively sinters or melts the powder particles fusing them together to form each individual layer.	A thermal extrusion, or a pressure extrusion of a thermoplastic, or a liquid material, respectively, which deposits and solidifies forming each individual layer.
Types	(1) Direct laser writing/Free surface printing (2) Mask-based laser writing/Constrained surface printing	(1) Binder jetting (2) Photopolymer jetting (3) Thermomaterial jetting	(1) Laser sintering (2) Laser melting	(1) Solid fibre extrusion (2) Liquid extrusion
Commercially available materials	Acrylonitrile-butadiene-styrene (ABS) and other proprietary epoxy or acrylate based photopolymers	**Binder jetting:** Ceramic, silica sand, stainless steel alloys, nickel alloys, iron alloys, chromium alloys, cobalt alloys, zircon, soda lime glass, and tungsten. **Photopolymer jetting:** Acrylonitrile-butadiene-styrene (ABS), and other proprietary epoxy or acrylate based photopolymers. **Thermomaterial jetting:** Wax and poly(methyl methacrylate) (PMMA).	**SLS:** Nylon, polyamide (PA), polyether ether ketone (PEEK), polyetherimide (PEI), polycarbonate (PC), polystyrene (PS), acrylonitrile-butadiene-styrene (ABS), polyester, polypropylene (PP), silica sand, thermoplastic polyurethane (TPU), and polyamide and nylon composites. **SLM:** Aluminium, cobalt-chromium alloys, copper alloys, gold, stainless steel, nickel alloys, silver, and titanium.	Polylactic acid (PLA), polycarbonate (PC), polystyrene (PS), acrylonitrile-butadiene-styrene (ABS), nylon, polyphenylsulfone (PPSF), polyetherimide (PEI), polyamide (PA), kevlar, acrylonitrile styrene acrylate (ASA), polyether ether ketone (PEEK), poly(methyl methacrylate) (PMMA), polyoxymethylene (POM), polypropylene (PP), poly(vinyl alcohol) (PVA), polyethylene terephthalate (PET), thermoplastic elastomers and polyurethanes, wax, and PLA composites (with carbon fibres, metals, magnetic irons, etc.)

	Stereolithography (SL)	Inkjet Printing	Selective Laser Sintering (SLS)	Fused Deposition Modeling (FDM)
Advantages	**Direct laser writing**: Exerts a low mechanical force on the building parts **Mask-based laser writing**: Enables high throughput printing, and the print height is independent of the reservoir height. **Common**: Offer high-resolution print capabilities, the process is free from solid support materials, and printed parts have a high optical transparency.	**Binder jetting:** Offers a wide variety of print materials. **Photopolymer and thermomaterial jetting:** Enable high throughput printing, offer multi-material and multi-colour printing capabilities, and allow fabrication of complex structures.	Availability of wide range of polymeric and metallic print materials, high purity and mechanical strength of the printed parts, and additional support material is not required.	Offers multi-material and multi-colour printing capabilities, low-cost printers and materials, availability of a wide variety of print materials, minimal post-processing requirements, and the use of miniaturised hand-held printing pens.
Limitations	**Direct laser writing**: Requires long print times, and the print height is dependent on the reservoir height. **Mask-based laser writing**: Exerts a high mechanical force on the building parts, allows limited flow of high viscosity resins, and the cured layer often sticks to the reservoir bottom surface. **Common**: Suffer from limited availability of print materials and limited multi-material print capabilities, and they often require a post photo-curing step.	**Binder jetting:** Offers a low-resolution print capability, physical and chemical properties of the printed parts are dictated by the binder, and printed parts suffer from material heterogeneities and bulk defects. **Photopolymer and thermomaterial jetting:** Suffer from limited availability of print materials, offer limited material customisation opportunities, and often require tedious post-processing steps.	The high cost of printers and materials, shrinkage and deformation of the printed parts, and a low throughput printing.	Printed parts suffer from material heterogeneities, bulk defects, low optical transparency, and staircase and chordal surface defects. It limits the fabrication of complex structures and usually emits hazardous fumes.

Selective laser sintering

Selective laser sintering/melting (SLS/M) techniques employ laser rastering on a powder bed to sinter or melt the required powder particles to fuse them together, as shown in Figure 1. An SLS/M process starts by rolling a layer of powder particles, which is then exposed to a laser as per the desired layer geometry. The laser increases the local bed temperature to either slightly below the melting point (for sintering) or above the melting point (for melting) of the powder particles. The sintered or melted powder particles fuse together to form the solid components of a layer, and the unfused particles act as a support material for the following layers. Completion of each individual layer is followed by lowering of the build platform and rising of the delivery platform by a specified step size, which is defined by the layer thickness. This allows the next layer of powder particles to be rolled down to repeat the same process for the consecutive layers, hence forming the desired 3D structure as shown in Figure 1. The final printed part is obtained from the powder bed, and it is post-processed to remove the unbound particles by dusting off with compressed air, blasting off with sand particles or glass beads, and/or taping and sonication.

As indicated above, the SLS 3D printing technique can be classified as selective laser sintering (SLS) or selective laser melting (SLM) techniques. As the name suggests, the former involves sintering of the powder particles (usually polymers), and the latter involves melting of the powder particles (usually metals). In both SLS and SLM techniques, the x and y resolution is dependent on the size of the powder particles and the laser spot, and the z resolution is dependent on the step size. These techniques offer various advantages, such as (1) the ability to print in a wide range of polymeric and metallic materials, (2) the high purity and high mechanical strength of the printed parts due to a strong thermal fusion between their each individual layers[16], and (3) they do not require any additional support material. These

techniques also suffer from a few limitations, such as (1) the higher cost of SLS/M printers and materials as compared to other 3D printing techniques, (2) the shrinkage and/or deformation of the printed parts, because of high thermal stress[17], and (3) a slow printing process.

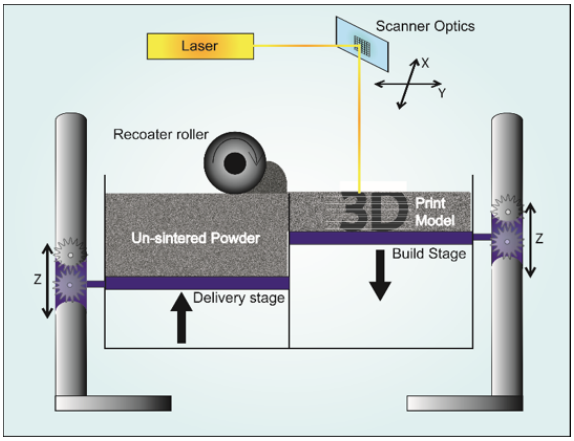

Figure 1. A schematic diagram of the selective laser sintering/melting printer.

Inkjet printing

3D inkjet printers are based on the similar principles to those of the most commonly used 2D inkjet printers. They both modulate the spatial and temporal jetting of inks from their respective print heads. However, 3D inkjet printer's print heads can supply a liquid binder, a photopolymer, or a thermomaterial on pre-specified spots in a layer-by-layer fashion. Based on the type of inks used, 3D inkjet printers can be classified as binder jetting, photopolymer jetting, or thermomaterial jetting printers.

Binder jetting printers are powder-based systems, similar to the SLS/M printers. Their print process begins by rolling a fine layer of powder from the powder bed onto the build platform with the help of rollers as shown in Figure 2 (a). The powder layer is then selectively exposed to a binder liquid as per the desired layer geometry. The binder liquid binds the required

powder particles together to form the solid components of a layer. The unbound powder particles act as a support material for the following layers. Completion of each individual layer is followed by lowering of the build platform and rising of the delivery platform by a specified step size, which is defined by the layer thickness. This allows the next layer of powder particles to be rolled down to repeat the same process for the consecutive layers, hence forming the desired 3D structure as shown in Figure 2 (a). The binder jetting printers offer an advantage that they allow the use of a wide variety of print materials (as listed in Table 1), because of their ability to use foreign binder liquids. However, they suffer from various limitations, such as (1) the x and y resolutions are dependent on the particle size of the powders (50 – 100 μm), and the z resolution is typically 200 μm[18], (2) the physical and chemical properties of the binders dominate the properties of the printed object, and (3) the printed objects suffer from material heterogeneity and bulk defects, because of the incomplete binding of powder particles, which limits their optical clarity and mechanical strength[19].

The photopolymer and thermomaterial jetting printers allow higher print resolution as compared to the binder jetting printers, because of their use of liquid precursors as opposed to the powder particles. These printers provide an x and y resolution of ca. 40 μm and a z resolution of ca. 16 μm[20]. A photopolymer or thermomaterial printing process starts with the jetting of build and support materials from their respective print heads as per the desired layer geometry. The jetted photopolymer or thermomaterial is UV polymerised or allowed to cool down on the build platform, respectively to form the solid components a layer. Completion of each individual layer is followed by lowering of the build platform to repeat the same process for the consecutive layers, hence forming the desired 3D structure as shown in Figure 2 (b). Moreover, these printers offer additional advantages, such as (1) the higher print speeds as

compared to the binder jetting printers, (2) ease of multi-material and multi-colour printing, via their ability to switch between different materials by using multiple print heads, (3) the ability to fabricate complex structures, from the use of dense support materials, and (4) the ability to fabricate mechanically more robust and optically more transparent parts, resulting from their better polymerisation and higher resolution capabilities as compared to the binder jetting printers. However, both photopolymer and thermomaterial jetting printers also suffer from a few limitations, such as (1) the limited availability of build materials, (2) the limited material customisation capabilities, because of the risk of blocking print heads, and (3) the requirement of long and tedious post-processing steps to remove the dense support material from complex geometries[21].

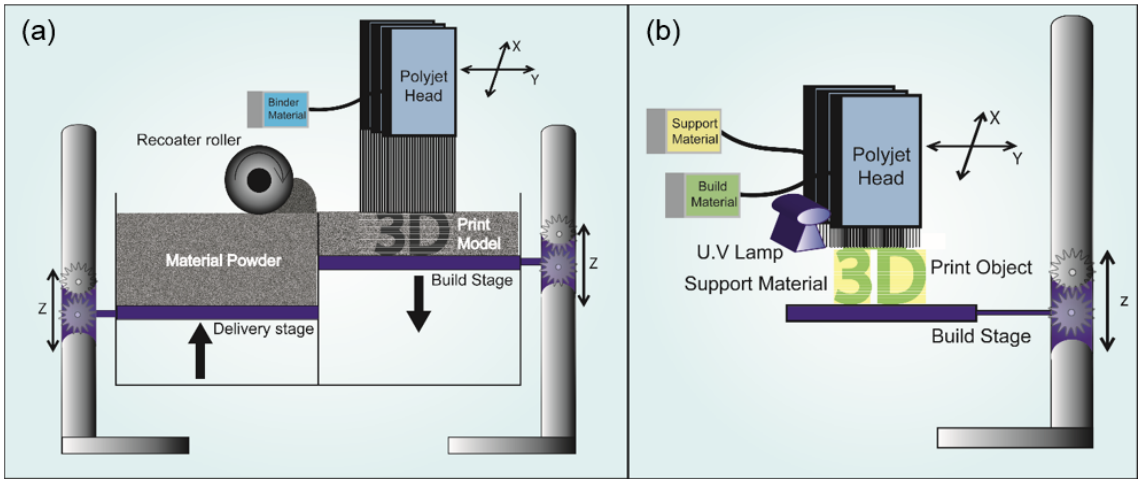

Figure 2. Schematic diagrams of inkjet printers: (a) binder jetting printer, (b) photopolymer jetting printer.

Most of the 3D printing techniques are only a decade or two old and are still in their relative infancy stages with respect to technological capabilities. However, they are rapidly evolving, and their capabilities and functionalities are being constantly improved. Some of the current limitations of different 3D printing techniques and the efforts that are being made towards

overcoming them are discussed below. This following section should help one to assess the current status and a future possible trajectory of the field of 3D printing.

Current status of the 3D printing techniques

Currently, the highest available 3D printing resolution is 50 μm in the x and y direction and 5 μm in the z direction with the use of SL printers, and it is many folds lower for the FDM (x, y, and z resolution of ca. 100 μm) and SLS (x, y, and z resolution of ca. 150 μm) printers. Note that depending on the geometry, the minimum possible size of a printed feature can be much larger than the specified print resolution. The resolution of different 3D printing techniques is being constantly improved, and a significant improvement in resolution has been observed especially for the SL and FDM printers over the past few years. The resolution of the SL printers can be further improved by using high definition projectors, reduction of the exposure light's focus depth, and optimisation of the exposure time, polymerisation wavelength, and printing power[22]. Improvements in the 3D printing resolution should allow (1) the ability to produce narrow channels, (2) higher optical transparency of the printed objects, and (3) reduction of the 'backside'[23] effect.

The most commonly used polymers with the FDM, SL, and PolyJet 3D printing techniques are currently limited to acrylates, acrylonitrile butadiene styrene (ABS), and poly(lactic acid) (PLA). However, the list of 3D printable materials is constantly increasing by incorporation of materials such as smart materials[24], nano-materials[25], composites[26], functional polymers[27], bioinks[28], hydrogels[29], and conductive materials[30]. FDM techniques allow the easiest use of a

customised material, which makes them a preferred choice to develop new customised materials.

Multi-material printing capabilities are currently only limited to the FDM and PolyJet printing techniques, however, efforts have also been made to allow similar capabilities with the SL printing techniques[31]. Multi-material printing can allow monolithic fabrication of objects that require simultaneous use of a variety of materials, such as anatomical models that require hard and elastic materials, optical components that require opaque and transparent materials, electronic components that require conductive and non-conductive materials, and educational models that require different coloured materials, to name but a few. Moreover, efforts are also being made to allow direct printing on foreign materials, such as cartilage printing on bones[32].

SL and PolyJet printed parts often suffer from poor biocompatibility. This is primarily due to the incomplete UV polymerisation, which leads to poor bonding, and hence leaching of toxic free radicles. The biocompatibility of these 3D printed polymeric parts is shown to be improved through post-curing steps[33]. Various commercial and non-commercial biocompatible materials have also been used for 3D printing, such as MED610 (Stratasys)[34] and hydrogels[29].

The fabrication of complex and long closed channels is still difficult with any of the above-mentioned 3D printing techniques. The FDM and SL printing techniques result in a collapse of long closed channels, because of the absence of any solid support material. Whereas, the PolyJet printing and SLS techniques result in a long post-processing time for the removal of

the solid support material from the closed channels[21]. Recently, water-soluble support materials such as SUP707 (Stratasys) (as described in Chapter 5) have been introduced to allow easier removal of the solid support material from the PolyJet printed parts.

All the health, environmental, and safety issues associated with different 3D printing techniques still remains to be explored, however, some concerning reports have been published recently[35]. 3D printing techniques such as FDM, which are most commonly and widely used in homes have been demonstrated to release harmful fumes during the printing process[36], and the disposal of SL and PolyJet printed parts has been demonstrated to be harmful to the environment[33, 37]. Accordingly, the need for standardisation and regulation of the 3D printing raw materials has been recognised[35]. However, the total assessment of the societal impact of 3D printing techniques still remains to be a topic of research and discussion[37].

Research aims

The research aims were (1) to obtain a better understanding of the capabilities and potential of different 3D printing techniques to fabricate three-dimensional micro- and milli-fluidic channels, (2) to investigate the effects of different three-dimensional channel arrangements on the performances of different miniaturised analytical devices, and (3) to use the obtained knowledge to develop new functional 3D printed miniaturised analytical devices (3D MADe).

Conventional fabrication techniques have inherently limited the production of miniaturised analytical devices to two-dimensional micro- and milli-fluidics. Moreover, these fabrication techniques have restricted the access of life-scientists and chemistry personnel to the microfluidic capabilities. As discussed above, 3D printing techniques can overcome these challenges while offering new possibilities and opportunities in the field of chemical sciences. However, there is limited understanding of the use of 3D printing techniques and three-dimensional fluidic channels in the field of chemical sciences, because of their relatively recent introduction. Accordingly, in this thesis, the use of 3D printing techniques and three-dimensional fluidics has been investigated with regard to the benefits they can offer in the production of miniaturised analytical devices. Furthermore, the use of 3D printing techniques has been studied to fabricate these devices using advanced materials such as titanium alloy (Ti-6Al-4V).

Throughout this thesis, several research questions have been addressed as some of them listed below: How currently available 3D printing capabilities can be used to fabricate functional miniaturised analytical devices? How do the choice of 3D printing technique and the build material affect the production and the performance of these devices? How can three-dimensional channel coiling be used to miniaturise analytical devices? How can three-dimensional channel arrangement be used to improve the performance of these miniaturised analytical devices? How does three-dimensional channel geometry can affect various hydrodynamic properties and hence functionalities of these devices? The knowledge and understanding gathered from these investigations are used to fabricate new functional 3D printed miniaturised analytical devices. Their use has been described to perform various analytical operations, such as liquid chromatographic separations and chemiluminescence detection. Moreover, computational fluid dynamic (CFD) simulations have been performed

for most of the developed three-dimensional fluidic designs to obtain a better understanding of the hydrodynamic properties of their respective analytical devices.

The work presented in this thesis should provide the groundwork for the future development of other 3D printed miniaturised analytical devices, and it should encourage the use of 3D printing techniques and three-dimensional fluidic channels in the wider fields of chemical sciences.

Overview of the thesis research chapters

Miniaturised liquid chromatographic columns can facilitate the production of portable high-performance liquid chromatographic (HPLC) systems. Currently, miniaturised chromatographic columns are fabricated by subtractive manufacturing techniques, such as dry and wet etching[38]. As discussed above, these techniques are limited to two-dimensional fabrication, and they use hazardous chemicals and/or processes. These limitations can be overcome with the use of 3D printing techniques to fabricate miniaturised capillary liquid chromatographic columns.

3D printing was previously used by Fee et al.[39] in 2014 to fabricate LC columns integrated with customised porous beds, internal flow distributors, and external fluid connectors. Furthermore, in the same year, Vonk et al.[40] had also reported 3D printed titanium-scaffolded narrow-bore columns to prevent the collapse of organic monoliths by fabricating titanium scaffolds within square conduits. However, the use of 3D printing techniques to fabricate coiled capillary chromatographic columns was not studied.

In Chapter 2, for the first time SLM 3D printing technique has been used to fabricate three-dimensionally coiled liquid chromatographic columns. The SLM technique was used to fabricate 600 mm long, 0.9 mm I.D. stainless steel (316L) and titanium alloy (Ti-6Al-4V) columns within a footprint of 5 × 30 × 30 mm. The work presented in Chapter 2 indicates the potential of SLM technique to fabricate miniaturised and robust liquid chromatographic columns.

This Chapter is published in the Analyst (2014, 139 (24), 6343-6347).

Currently, SLM techniques suffer from a low printing resolution as described above. This resulted in a low chromatographic performance of the slurry packed LC columns, because of their high (20 μm) channel wall roughness, as also described in Chapter 2.

In Chapter 3, the use of titanium wall bonded organic monolith is described to circumvent the limitation of channel wall roughness, and hence produce the first functional 3D printed coiled liquid chromatographic column. The SLM technique was used to fabricate a titanium alloy (Ti-6Al-4V) column, which was functionalised with in-column thermally polymerised and wall bonded poly(BuMA-*co*-EDMA) monolith. Titanium was selected as a suitable candidate for the fabrication of monolithic chromatographic columns because of its favourable chemical properties and high thermal conductivity. Thermally oxidised titanium channel walls were silanised to form a stable covalent bond with the acrylate monolith. The work presented in Chapter 3 indicates that 3D printed titanium columns with wall bonded organic monoliths can be used for (1) liquid chromatographic separations of proteins and peptides

and (2) generating rapid bi-directional heating/cooling cycles for steep temperature gradient liquid chromatographic separations.

This Chapter is published in the Analytica Chimica Acta (2016, 910, 84-94).

In Chapter 4, the first study of the effect of 3D column geometry on liquid chromatographic separations in the presence of a stationary phase is described. The effect of column geometry on the chromatographic efficiency, particularly in the case of packed and monolithic columns, and more particularly in the case of liquid chromatographic separations has remained unclear. Accordingly, three chromatographic column geometries, namely (i) a 2D serpentine, (ii) a 3D spiral, and (iii) a novel 3D serpentine were developed to study these effects. Chapter 4 describes (1) their functionalisation with in-column thermally polymerised poly(BuMA-*co*-EDMA) monoliths, (2) their comparative performances for liquid chromatographic separations of small and large molecules, (3) insights into the effect of column geometry using computational fluid dynamic (CFD) simulations, and (4) their liquid chromatographic separation efficiencies under isocratic and gradient conditions.

This Chapter is published in the Analytical Chemistry (DOI:10.1021/acs.analchem.7b03778).

Chemiluminescence detection (CLD) systems require simple instrumentation and provide extremely high sensitivity for at least some analytes, which makes them a suitable candidate for miniaturised analytical devices. A Flow-cell plays a significant role in determining the sensitivity and reproducibility of the CLD systems. Usually, CLD flow-cells are fabricated by coiling polymeric or glass tubing in a plane[41-42] or by milling/etching channels into polymeric materials [43-46]. Coiling polymeric or glass tubing limit the flow-cell design to predominantly

flat spirals due to their rigid nature[47]. Whereas, milling/etching techniques require an additional channel sealing procedure, lack three-dimensional fabrication, and require time and labour intensive steps. These limitations can be overcome with the use of 3D printing techniques to fabricate CLD flow-cells.

PolyJet 3D printing technique was first used for the fabrication of CLD flow-cells by Spilstead et al.[21] in 2014. However, this preliminary investigation used the conventional spiral flow-cell design. The use of coiled spiral flow-cell design resulted in channels with only partially cleared support material and hence led to significant flow-cell staining. In order to obtain clear channels, open channels were printed, which were later sealed with transparent films[21]. This requires design and fabrication of a new less convoluted flow-cell design to allow successful PolyJet printing of closed channel flow-cells.

In Chapter 5, design and development of a new and improved CLD flow-cell is described. The new flow-cell was designed by diverging multiple linear channels from a common centre port in a radial arrangement, and hence it was named as a 'radial' flow-cell. Fabrication of this flow-cell with the PolyJet printing and FDM techniques was studied. Chapter 5 describes the design, development, and evaluation of the radial flow-cell by (1) comparing its ease of fabrication and CLD performance with its counterpart 3D printed and polymer tubing spiral flow-cells, (2) investigating its fluidic properties through CFD simulations, and (3) developing a rapid and automated assay for the analysis of H_2O_2 in urine and coffee extract samples.

This Chapter is published in the Analytica Chimica Acta (DOI: 10.1016/j.aca.2017.12.039).

REFERENCES

1. Hwang, H.; Kim, Y.; Cho, J.; Lee, J.-y.; Choi, M.-S.; Cho, Y.-K., Lab-on-a-disc for simultaneous determination of nutrients in water. *Analytical chemistry* **2013,** *85* (5), 2954-2960.
2. Shu, B.; Zhang, C.; Xing, D., Highly sensitive identification of foodborne pathogenic Listeria monocytogenes using single-phase continuous-flow nested PCR microfluidics with on-line fluorescence detection. *Microfluidics and nanofluidics* **2013,** *15* (2), 161-172.
3. Piorek, B. D.; Lee, S. J.; Moskovits, M.; Meinhart, C. D., Free-surface microfluidics/surface-enhanced Raman spectroscopy for real-time trace vapor detection of explosives. *Analytical chemistry* **2012,** *84* (22), 9700-9705.
4. Reboud, J.; Bourquin, Y.; Wilson, R.; Pall, G. S.; Jiwaji, M.; Pitt, A. R.; Graham, A.; Waters, A. P.; Cooper, J. M., Shaping acoustic fields as a toolset for microfluidic manipulations in diagnostic technologies. *Proceedings of the National Academy of Sciences* **2012,** *109* (38), 15162-15167.
5. Karande, A. D.; Heng, P. W. S.; Liew, C. V., In-line quantification of micronized drug and excipients in tablets by near infrared (NIR) spectroscopy: Real time monitoring of tabletting process. *International journal of pharmaceutics* **2010,** *396* (1), 63-74.
6. Rogers, C. I.; Qaderi, K.; Woolley, A. T.; Nordin, G. P., 3D printed microfluidic devices with integrated valves. *Biomicrofluidics* **2015,** *9* (1), 016501.
7. Hull, C. W., Apparatus for production of three-dimensional objects by stereolithography. Google Patents: 1986.
8. Peltola, S. M.; Melchels, F. P.; Grijpma, D. W.; Kellomäki, M., A review of rapid prototyping techniques for tissue engineering purposes. *Annals of medicine* **2008,** *40* (4), 268-280.
9. Murphy, S. V.; Atala, A., 3D bioprinting of tissues and organs. *Nature biotechnology* **2014,** *32* (8), 773-785.
10. Marks, P., 3D printing takes off with the world's first printed plane. *NewScientist* **2011,** *211* (2823), 17-18.
11. Bartlett, N. W.; Tolley, M. T.; Overvelde, J. T.; Weaver, J. C.; Mosadegh, B.; Bertoldi, K.; Whitesides, G. M.; Wood, R. J., A 3D-printed, functionally graded soft robot powered by combustion. *Science* **2015,** *349* (6244), 161-165.
12. Allard, T.; Sitchon, M.; Sawatzky, R.; Hoppa, R. In *Use of hand-held laser scanning and 3d printing for creation of a museum exhibit*, 6th International Symposium on Virtual Reality, Archaelogy and Cultural Heritage, 2005.
13. Sun, J.; Peng, Z.; Zhou, W.; Fuh, J. Y.; Hong, G. S.; Chiu, A., A review on 3D printing for customized food fabrication. *Procedia Manufacturing* **2015,** *1*, 308-319.
14. McDonald, J. C.; Chabinyc, M. L.; Metallo, S. J.; Anderson, J. R.; Stroock, A. D.; Whitesides, G. M., Prototyping of microfluidic devices in poly (dimethylsiloxane) using solid-object printing. *Analytical chemistry* **2002,** *74* (7), 1537-1545.
15. Gross, B. C.; Erkal, J. L.; Lockwood, S. Y.; Chen, C.; Spence, D. M., Evaluation of 3D printing and its potential impact on biotechnology and the chemical sciences. *Analytical chemistry* **2014,** *86* (7), 3240-3253.
16. Gupta, V.; Talebi, M.; Deverell, J.; Sandron, S.; Nesterenko, P. N.; Heery, B.; Thompson, F.; Beirne, S.; Wallace, G. G.; Paull, B., 3D printed titanium micro-bore columns containing polymer monoliths for reversed-phase liquid chromatography. *Analytica chimica acta* **2016,** *910*, 84-94.
17. Wang, R.-J.; Wang, L.; Zhao, L.; Liu, Z., Influence of process parameters on part shrinkage in SLS. *The International Journal of Advanced Manufacturing Technology* **2007,** *33* (5), 498-504.
18. Pfister, A.; Landers, R.; Laib, A.; Hübner, U.; Schmelzeisen, R.; Mülhaupt, R., Biofunctional rapid prototyping for tissue-engineering applications: 3D bioplotting versus 3D printing. *Journal of Polymer Science Part A: Polymer Chemistry* **2004,** *42* (3), 624-638.
19. Gross, B. C.; Erkal, J. L.; Lockwood, S. Y.; Chen, C.; Spence, D. M., Evaluation of 3D printing and its potential impact on biotechnology and the chemical sciences. ACS Publications: 2014.

20. de Gans, B. J.; Duineveld, P. C.; Schubert, U. S., Inkjet printing of polymers: state of the art and future developments. *Advanced materials* **2004,** *16* (3), 203-213.
21. Spilstead, K. B.; Learey, J. J.; Doeven, E. H.; Barbante, G. J.; Mohr, S.; Barnett, N. W.; Terry, J. M.; Hall, R. M.; Francis, P. S., 3D-printed and CNC milled flow-cells for chemiluminescence detection. *Talanta* **2014,** *126*, 110-115.
22. Donvito, L.; Galluccio, L.; Lombardo, A.; Morabito, G.; Nicolosi, A.; Reno, M., Experimental validation of a simple, low-cost, T-junction droplet generator fabricated through 3D printing. *Journal of Micromechanics and Microengineering* **2015,** *25* (3), 035013.
23. Waldbaur, A.; Rapp, H.; Laenge, K.; Rapp, B. E., Let there be chip—towards rapid prototyping of microfluidic devices: one-step manufacturing processes. *Analytical Methods* **2011,** *3* (12), 2681-2716.
24. Ahn, S.-H.; Lee, K.-T.; Kim, H.-J.; Wu, R.; Kim, J.-S.; Song, S.-H., Smart soft composite: An integrated 3D soft morphing structure using bend-twist coupling of anisotropic materials. *International Journal of Precision Engineering and Manufacturing* **2012,** *13* (4), 631-634.
25. Ahn, B. Y.; Duoss, E. B.; Motala, M. J.; Guo, X.; Park, S.-I.; Xiong, Y.; Yoon, J.; Nuzzo, R. G.; Rogers, J. A.; Lewis, J. A., Omnidirectional printing of flexible, stretchable, and spanning silver microelectrodes. *Science* **2009,** *323* (5921), 1590-1593.
26. Kalsoom, U.; Nesterenko, P. N.; Paull, B., Recent developments in 3D printable composite materials. *RSC Advances* **2016,** *6* (65), 60355-60371.
27. Nadgorny, M.; Xiao, Z.; Chen, C.; Connal, L. A., Three-Dimensional Printing of pH-Responsive and Functional Polymers on an Affordable Desktop Printer. *ACS applied materials & interfaces* **2016,** *8* (42), 28946-28954.
28. Colosi, C.; Shin, S. R.; Manoharan, V.; Massa, S.; Costantini, M.; Barbetta, A.; Dokmeci, M. R.; Dentini, M.; Khademhosseini, A., Microfluidic Bioprinting of Heterogeneous 3D Tissue Constructs Using Low-Viscosity Bioink. *Advanced Materials* **2016,** *28* (4), 677-684.
29. Hockaday, L.; Kang, K.; Colangelo, N.; Cheung, P.; Duan, B.; Malone, E.; Wu, J.; Girardi, L.; Bonassar, L.; Lipson, H., Rapid 3D printing of anatomically accurate and mechanically heterogeneous aortic valve hydrogel scaffolds. *Biofabrication* **2012,** *4* (3), 035005.
30. Li, J.; Ye, F.; Vaziri, S.; Muhammed, M.; Lemme, M. C.; Östling, M., Efficient inkjet printing of graphene. *Advanced materials* **2013,** *25* (29), 3985-3992.
31. Zhou, C.; Chen, Y.; Yang, Z.; Khoshnevis, B. In *Development of multi-material mask-image-projection-based stereolithography for the fabrication of digital materials*, Annual solid freeform fabrication symposium, Austin, TX, 2011.
32. D O'Connell, C.; Di Bella, C.; Thompson, F.; Augustine, C.; Beirne, S.; Cornock, R.; Richards, C. J.; Chung, J.; Gambhir, S.; Yue, Z., Development of the Biopen: a handheld device for surgical printing of adipose stem cells at a chondral wound site. *Biofabrication* **2016,** *8* (1), 015019.
33. Oskui, S. M.; Diamante, G.; Liao, C.; Shi, W.; Gan, J.; Schlenk, D.; Grover, W. H., Assessing and reducing the toxicity of 3D-printed parts. *Environmental Science & Technology Letters* **2015,** *3* (1), 1-6.
34. Sayyar, S.; Murray, E.; Thompson, B.; Chung, J.; Officer, D. L.; Gambhir, S.; Spinks, G. M.; Wallace, G. G., Processable conducting graphene/chitosan hydrogels for tissue engineering. *Journal of Materials Chemistry B* **2015,** *3* (3), 481-490.
35. Jeremy, F.; Cindy, B.; Suraj, B.; Myles, I., Comparing environmental impacts of additive manufacturing vs traditional machining via life-cycle assessment. *Rapid Prototyping Journal* **2015,** *21* (1), 14-33.
36. Bharti, N., 3D Printing in Makerspaces: Health and Safety Concerns. *Issues in Science and Technology Librarianship* **2017**.
37. Huang, S. H.; Liu, P.; Mokasdar, A.; Hou, L., Additive manufacturing and its societal impact: a literature review. *The International Journal of Advanced Manufacturing Technology* **2013**, 1-13.
38. Terry, S. C.; Jerman, J. H.; Angell, J. B., A gas chromatographic air analyzer fabricated on a silicon wafer. *IEEE Transactions on Electron Devices* **1979,** *26* (12), 1880-1886.

39. Fee, C.; Nawada, S.; Dimartino, S., 3D printed porous media columns with fine control of column packing morphology. *Journal of Chromatography A* **2014,** *1333*, 18-24.
40. Vonk, R. J.; Vaast, A.; Eeltink, S.; Schoenmakers, P. J., Titanium-scaffolded organic-monolithic stationary phases for ultra-high-pressure liquid chromatography. *Journal of Chromatography A* **2014,** *1359*, 162-169.
41. Burguera, J.; Townshend, A.; Greenfield, S., Flow injection analysis for monitoring chemiluminescent reactions. *Analytica Chimica Acta* **1980,** *114*, 209-214.
42. Campıns-Falcó, P.; Tortajada-Genaro, L.; Bosch-Reig, F., A new flow cell design for chemiluminiscence analysis. *Talanta* **2001,** *55* (2), 403-413.
43. Nakamura, H.; Murakami, Y.; Yokoyama, K.; Tamiya, E.; Karube, I.; Suda, M.; Uchiyama, S., A compactly integrated flow cell with a chemiluminescent FIA system for determining lactate concentration in serum. *Analytical chemistry* **2001,** *73* (2), 373-378.
44. Tyrrell, É.; Gibson, C.; MacCraith, B. D.; Gray, D.; Byrne, P.; Kent, N.; Burke, C.; Paull, B., Development of a micro-fluidic manifold for copper monitoring utilising chemiluminescence detection. *Lab on a Chip* **2004,** *4* (4), 384-390.
45. Guan, Y.-X.; Xu, Z.-R.; Dai, J.; Fang, Z.-L., The use of a micropump based on capillary and evaporation effects in a microfluidic flow injection chemiluminescence system. *Talanta* **2006,** *68* (4), 1384-1389.
46. Terry, J. M.; Adcock, J. L.; Olson, D. C.; Wolcott, D. K.; Schwanger, C.; Hill, L. A.; Barnett, N. W.; Francis, P. S., Chemiluminescence detector with a serpentine flow cell. *Analytical chemistry* **2008,** *80* (24), 9817-9821.
47. Terry, J. M.; Zammit, E. M.; Slezak, T.; Barnett, N. W.; Olson, D. C.; Wolcott, D. K.; Edwards, D. L.; Francis, P. S., Solution mixing and the emission of light in flow-cells for chemiluminescence detection. *Analyst* **2011,** *136* (5), 913-919.

Chapter 2:

3D PRINTED METAL COLUMNS FOR CAPILLARY LIQUID CHROMATOGRAPHY

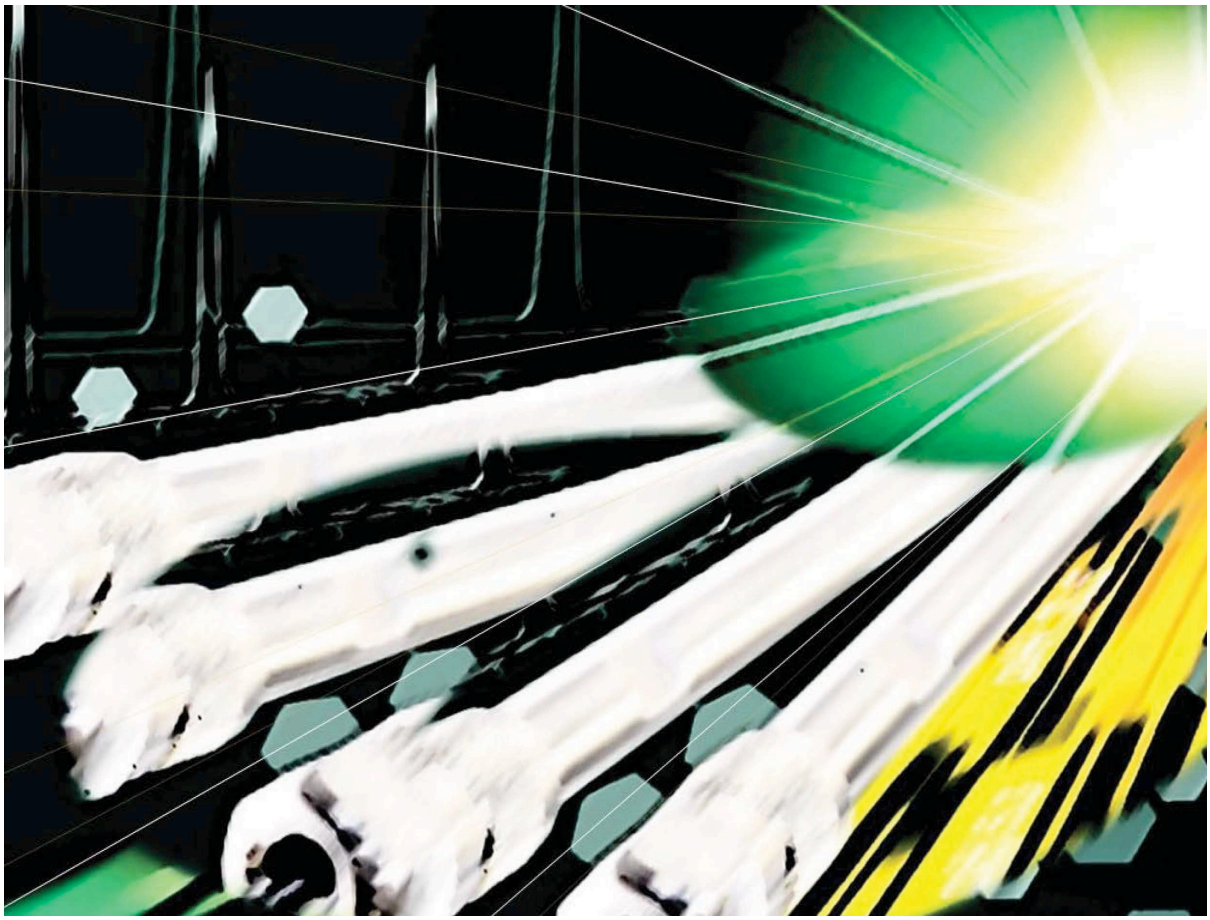

Chapter 2 has been removed for copyright or proprietary reasons.

(As published in the Analyst 2014, 139 (24), 6343-6347)

Chapter 3:

3D PRINTED TITANIUM MICRO-BORE COLUMNS CONTAINING POLYMER MONOLITHS FOR REVERSED-PHASE LIQUID CHROMATOGRAPHY

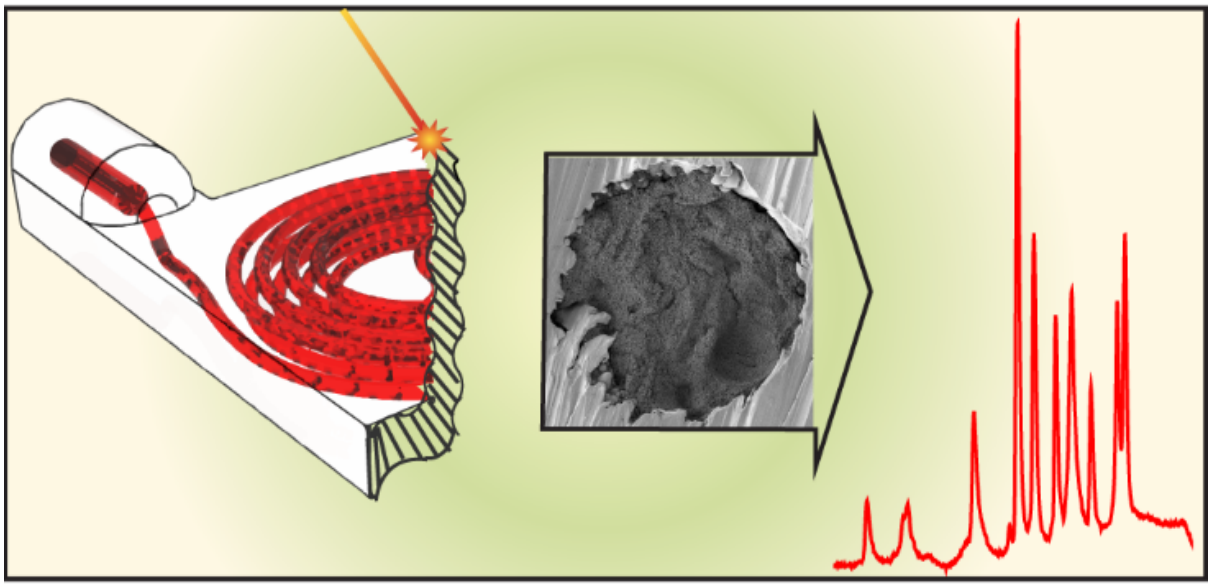

(As published in the Analytica Chimica Acta 2016, 910, 84-94)

Chapter 3 has been removed for copyright or proprietary reasons.

Chapter 4:

INVESTIGATING THE EFFECT OF COLUMN GEOMETRY ON SEPARATION EFFICIENCY USING 3D PRINTED LIQUID CHROMATOGRAPHIC COLUMNS CONTAINING POLYMER MONOLITHIC PHASES

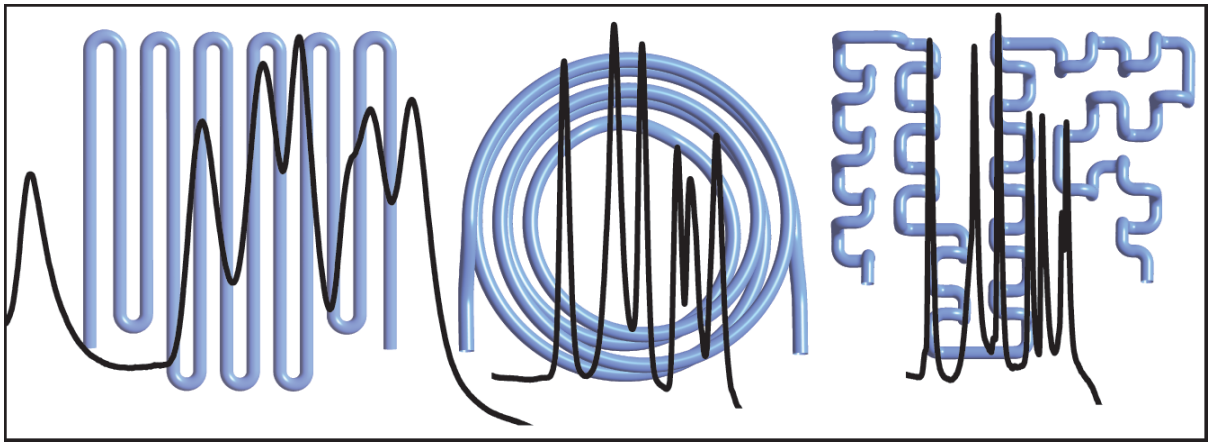

(As published in the Analytical Chemistry DOI: 10.1021/acs.analchem.7b03778)

Chapter 4 has been removed for copyright or proprietary reasons.

Chapter 5:

A NEW 3D PRINTED RADIAL FLOW-CELL FOR CHEMILUMINESCENCE DETECTION: APPLICATION IN ION CHROMATOGRAPHIC DETERMINATION OF HYDROGEN PEROXIDE IN URINE AND COFFEE EXTRACTS

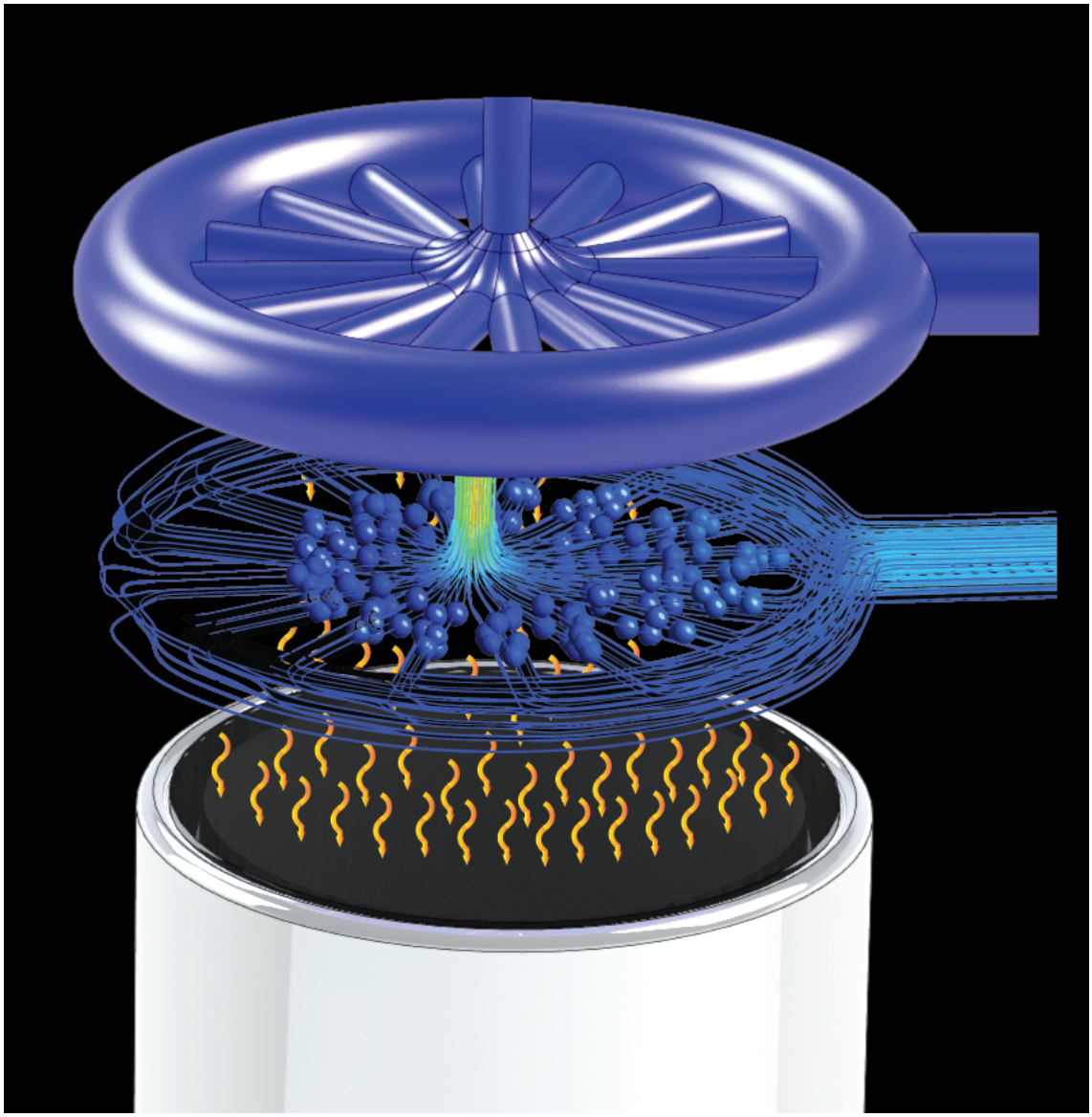

(As published in the Analytica Chimica Acta DOI: 10.1016/j.aca.2017.12.039)

Chapter 5 has been removed for copyright or proprietary reasons.

Chapter 6:

CONCLUSIONS AND FUTURE OUTLOOK

The use of 3D printing techniques to fabricate three-dimensional micro- and milli-fluidic, miniaturised, and functional metallic and polymeric analytical devices has been explored. The SLM 3D printing technique has been used for the first time to fabricate metallic capillary liquid chromatographic columns. The PolyJet 3D printing technique has been used for the first time to successfully fabricate a chemiluminescence detection flow-cell.

As described in Chapters 2-4, previously impractical column geometries, such as double handed coiled spiral and three-dimensionally convoluted serpentine can be readily fabricated with the use of 3D printing techniques. Moreover, 3D printing techniques such as SLM, allow their fabrication in metal, including high strength titanium alloys. SLM technique has been used to fabricate 0.9 mm I.D. columns with following geometries (1) a 600 mm long double-handed coiled 3D spiral, (2) a 300 mm long 3D serpentine, (3) a 300 mm long single handed 3D spiral, and (4) a 300 mm long 2D serpentine within a footprint of ca. 30 X 30 X 5 mm as described in Chapters 2-4. Furthermore, a 0.9 I.D. and 5000 mm long column with nested helix column geometry has also been fabricated within a footprint of 30 X 30 X 30 mm for future investigations. Long chromatographic columns are frequently used to obtain high-efficiency liquid and gas chromatographic separations. However, their resulting large footprints often render their integration into miniaturised platforms cumbersome and ineffective. The here described fabrication of long capillary columns within small footprints

using 3D printing techniques can provide an opportunity to allow easy access to long chromatographic columns for the miniaturised chromatographic platforms.

Chapter 4 describes the use of 3D printing techniques to perform challenging investigations, such as the effects of 3D column geometries on chromatographic separation efficiencies. 3D printing techniques allowed the fabrication of precisely controlled column geometries to probe the long-debated but experimentally unobserved effects of column coiling on the liquid chromatographic separations. 3D printing techniques allow the fabrication of complex fluidic geometries, and CFD simulations allow the study of hydrodynamic properties in those complex geometries. As described in Chapters 4 and 5, an amalgamation of these capabilities can be used to perform fundamental studies in the field of microfluidics.

As described in Chapters 2-4, an in-house built Peltier thermoelectric modules based direct contact heating/cooling system has been used for liquid chromatographic separations. It enabled the substitution of conventional cumbersome HPLC column ovens with a low-cost, miniaturised, and bi-directional temperature modulation system. Moreover, it allowed (1) near real-time bidirectional column temperature modulation, (2) precise temperature regulation, and (3) the generation of inverse temperature gradients. Similar assemblies based on Peltier modules should allow easy access to bi-directional temperature regulation units for miniaturised analytical platforms.

The wall bonding of the organic (acrylate) monolith with the inorganic (titanium) channel walls through silanisation has enabled a conformal in-column monolith polymerisation in all the here-studied column geometries as described in Chapters 3 and 4. This demonstrates

fabrication of uniform monolithic stationary phases even in micro-bore, highly convoluted, and rough channel wall columns. This should further encourage the use of monolithic stationary phases in other similar applications where particle packing procedures usually result in an unsatisfactory performance.

As described in Chapter 5, the PolyJet 3D printing technique has been used to fabricate a new radial chemiluminescence detection flow-cell by three-dimensional arrangement of microfluidic channels. Moreover, this was the first time that a 3D printing technique was successfully used to fabricate a chemiluminescence detection flow-cell. The developed radial flow-cell design allowed (1) rapid and easy fabrication with the PolyJet and FDM 3D printing techniques and (2) higher efficiency chemiluminescence detection of H_2O_2 using the luminol-Co(II) chemiluminescence reagent as compared to the conventional spiral flow-cell design. The PolyJet 3D printed radial flow-cell was further used in an IC-CLD system to determine H_2O_2 (a biomarker) in human urine and coffee extract samples. The here demonstrated ability of 3D printing techniques to produce rapid, low-cost, and customisable chemiluminescence detection flow-cells should allow its use to fabricate similar flow-cells for in-house built and commercial chemiluminescence detection systems.

The work presented in this thesis demonstrates the use of 3D printing techniques, namely SLM and PolyJet printing to directly fabricate metallic (stainless steel and titanium) and polymeric (acrylate) three-dimensional micro- and milli-fluidic devices. These devices have been used to perform analytical operations such as liquid chromatographic separations and chemiluminescence detection. Moreover, the use of CFD simulation capabilities along with the 3D printing capabilities allowed (1) an investigation into the long-standing question of the

effect of column geometry on liquid chromatographic separations and (2) the optimisation and investigation of a new radial chemiluminescence detection flow-cell design. The work presented here should encourage and inspire other researchers to fabricate other functional 3D printed miniaturised analytical devices and use three-dimensional micro- and milli-fluidic channels in the wider fields of chemical sciences.